Earthquake Geotechnical Engineering for Protection and Development of Environment and Constructions – Silvestri & Moraci (Eds)
© 2019 Associazione Geotecnica Italiana, Rome, Italy, ISBN 978-0-367-14328-2

The effects of uncertainty of soil properties on the estimation of seismic ground settlements for unsaturated sandy soils

T. Kitazume
Tokyo Electric Power Services Co., Ltd., Tokyo, Japan

S. Goto
S. GotoUniversity of Yamanashi, Kofu, Japan

ABSTRACT: With the help of some torsional cyclic shear tests, we determined volumetric strain of unsaturated sandy soils subject to cyclic shear under exhaust drainage conditions. Based on the results of implementing a few cases where we changed dry density and moisture content, it came to light that smaller is dry density, higher is volumetric strain; higher is moisture content, higher is volumetric strain; and percentage change in volumetric strain due to fluctuation in these physical properties differ according to shear stress ratio. We conducted reliability analysis related to the estimation of seismic ground settlements considering the variation in dry density and moisture content, and we plotted fragility curves of seismic ground settlements.

By the way, the method is based on the cumulative damage analysis in which shear stress time histories based on seismic response analysis of the ground are taken into consideration. Such an estimated method of settlement depends on the precision of seismic response analysis. Therefore, we estimated settlement using four different seismic response analyses and considered about the modeling error from differences between those estimates and actual survey settlements. We show the composite fragility curve that added a modeling error to a fragility curve in considering the variation in dry density and moisture content.

1 INTRODUCTION

1.1 *Background*

We have conducted hollow torsional cyclic shear tests (stress-controlled method) under exhausted air and drained conditions on unsaturated sandy soil ground at the site of Tokyo Electric Power Company's Kashiwazaki-Kariwa Nuclear Plant. This site underwent ground settlements during the 2007 Niigata-ken Chuetsu-oki Earthquake (Sakai et al. 2009). From the test results, we determined the relationship among the number of cycles, shear stress, and volumetric strain (equivalent volumetric strain curves) (Figure 1a). Additionally, we estimated the amount of settlements by applying the time history of shear stress obtained from the seismic response analysis to the equivalent volumetric strain curves based on the cumulative damage analysis (Figure 1b). The estimated amount of settlements generally fits the actual measurement value (Kitazume et al. 2015). To apply the proposed method to predictive evaluations, the variability of the ground material characteristic values and differences among earthquake response analysis methods must also be considered.

1.2 *Purpose*

This paper discusses three items. 1) The dry density and moisture content are used as physical properties of unsaturated sandy ground that affects the amount of settlements during an earthquake. We compared and organized the volumetric strain of the average physical properties as

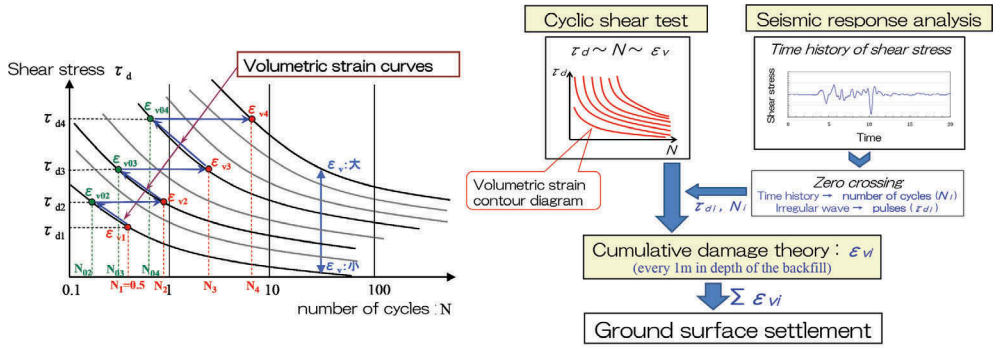

(a) Volumetric strain curves (b) Settlement calculation flow chart

Figure 1. Volumetric strain curves and Settlement calculation flow chart

functions of dry density and moisture content, and showed their correlation relationship. 2) Reliability analysis of the estimated amount of settlements during an earthquake is conducted while accounting for the variability of dry density and moisture content. We evaluated the results as the fragility curve for the susceptibility to settlements of unsaturated sandy ground during earthquakes. 3) The amount of settlements is estimated using several different earthquake response analysis methods. Then we compared the difference from the actual measured amount of the settlements during an earthquake and analyzed the modeling errors in each method.

2 VARIABILITY OF THE PHYSICAL PROPERTIES

2.1 *Relation between dry density and moisture content, and volumetric strain*

We conducted hollow torsional cyclic shear test under exhaust drainage conditions. on the sample having 1.60 g/cm^3 average initial dry density and 10 % initial moisture content, and samples with 20 % average initial moisture content and initial dry density of 1.52 and 1.70 g/cm^3 respectively. Confining pressure was σ'_m = 100 kPa. Table 1 shows the list of test

Table 1. Test conditions of torsional cyclic shear test and volumetric strain at *N20* and *N50*

Test number	Initial dry density ρ_{d0} (g/m^3)	Initial moisture content w_0 (%)	Confining pressure σ'_m (kPa)	Shear stress ratio $SR_d = \tau_d/\sigma'_m$	Volumetric strain ε_{v_N20} (%)	Volumetric strain ε_{v_N50} (%)
1-1	1.60*	20*	100	0.26	0.444	0.708
1-2				0.39	1.199	1.689
1-3				0.52	2.814	3.499
1-4				0.60	3.630	4.441
2-1	1.60	10	100	0.26	0.212	0.276
2-2				0.41	0.533	0.647
2-3				0.52	0.854	1.067
2-4				0.62	1.607	2.047
3-1	1.52	20	100	0.25	0.961	1.363
3-2				0.41	2.269	3.122
3-3				0.51	4.409	5.308
4-1	1.70	20	100	0.37	1.072	1.404
4-2				0.51	1.591	1.856
4-3				0.60	1.833	2.087

* Average physical properties

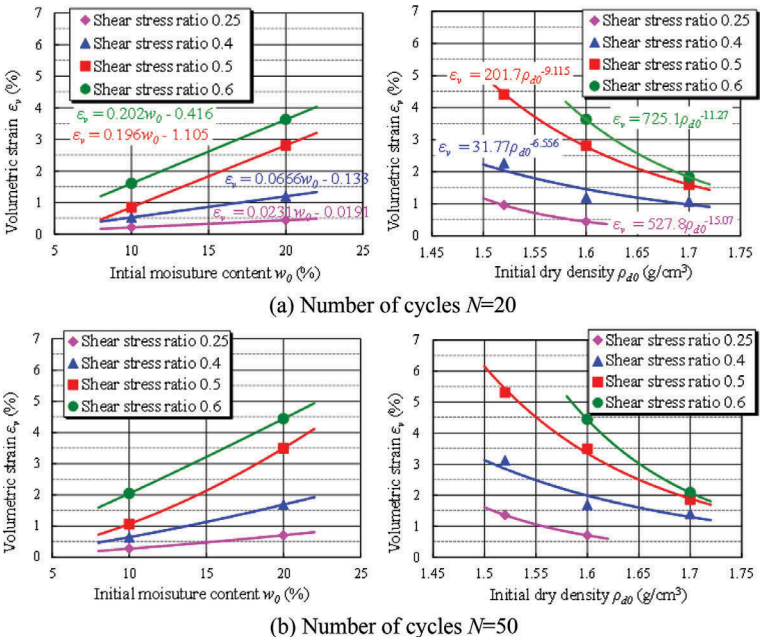

Figure 2. Relation between moisture content and dry density, and volumetric strain

conditions and volumetric strain (ε_{v_N20}, ε_{v_N50}) for 20 and 50 cycles respectively. From Table 1, it is clear that volumetric strain for *N50* is 2-3 times of that for *N20*.

With respect to the relation between initial moisture content and volumetric strain, and the relation between initial dry density and volumetric strain, Figure 2 shows the comparison results for each shear stress ratio. From this figure, it can be confirmed that if shear stress ratio differs, percentage change in volumetric strain with respect to change in initial dry density and initial moisture content also differs.

2.2 *Setting correlation*

From the aforementioned data, it was confirmed that volumetric strain of unsaturated sandy soils subject to cyclic shear differs according to difference in physical properties such as initial dry density (ρ_{d0}) and initial moisture content (w_0). Therefore, in this section, for evaluating seismic ground settlements level considering variation in ground characteristics described later, we will specify the relation between these physical properties and volumetric strain.

In the first place, we will set coefficient α_1 that defines the relation between initial dry density (ρ_{d0}) and volumetric strain. With respect to the relational expression of initial dry density and volumetric strain by shear stress ratio (τ_d/σ'_m) for the number of cycles N = 20 shown in the left figure of Figure 2a, we standardize with the volumetric strain that occurs at each average initial dry density and set as follows.

$$\begin{aligned}
\alpha_1 &= 725.05 \cdot {\rho_{d0}}^{-11.27}/3.63 \ (\tau_d/\sigma'_m > 0.55) \\
\alpha_1 &= 201.67 \cdot {\rho_{d0}}^{-9.115}/2.81 \ (0.55 \geq \tau_d/\sigma'_m > 0.45) \\
\alpha_1 &= 31.765 \cdot {\rho_{d0}}^{-6.556}/\ 1.20 \ (0.45 \geq \tau_d/\sigma'_m > 0.325) \\
\alpha_1 &= 527.80 \cdot {\rho_{d0}}^{-15.07}/\ 0.444 \ (0.325 \geq \tau_d/\sigma'_m)
\end{aligned} \tag{1}$$

Next, we will set coefficient α_2 that defines relation between initial moisture content (w_0) and volumetric strain. With respect to the relational expression of initial moisture content and volumetric strain for each shear stress ratio (τ_d/σ'_m) for the number of cycles N = 20 shown in

the right figure in Figure 2(a), we standardize with the volumetric strain that occurs at each average initial moisture content and set as follows.

$$\begin{aligned}
\alpha_2 &= (0.202 \cdot w_0 - 0.416)/3.63 \ (\tau_d/\sigma_m{}' > 0.55) \\
\alpha_2 &= (0.196 \cdot w_0 - 1.105)/2.81 \ (0.55 \geq \tau_d/\sigma_m{}' > 0.45) \\
\alpha_2 &= (0.0666 \cdot w_0 - 0.133)\ /1.20 \ (0.45 \geq \tau_d/\sigma_m{}' > 0.325) \\
\alpha_2 &= (0.0231 \cdot w_0 - 0.0191)\ /\ 0.444 \ (0.325 \geq \tau_d/\sigma_m{}')
\end{aligned} \tag{2}$$

Formula (1) and (2) used the middle values (0.55, 0.45 and 0.325) of the experimental conditions (τ_d/σ'_m = 0.6, 0.5, 0.4, 0.25) as the range of the shear stress ratio.

We applied the correlation equation at the number of cycles N = 20 based on the number of cycles where we get zero cross for amplitude of the main moving part in the seismic movement used in this study (Kitazume et al.2015). When the number of cycles N = 20 (the left figure in Figure 2a), only two data points describe the initial moisture content. Thus, the relationship between the initial moisture content and volumetric strain is expressed linearly. Nevertheless, a convex curvature is obtained for N = 50 (the left figure in Figure 2b), and the compaction test shows the existence of the optimal moisture content. Therefore, the graph is expected to exhibit a curvature with a local minimum point.

In the present study, by multiplying volume strain arising based on the average physical properties (ρ_{d0} = 1.60 g/cm^3, and w_0 = 20%) with coefficients α_1 and α_2, we presented a recursive method that allows to easily set the volumetric strain when initial dry density or initial moisture content has varied. Correlations shown in formula (1) and (2) are specific to ground at the points covered in the present study, and they are not generic in nature.

3 EVALUATION OF THE AMOUNT OF SETTLEMENTS WHILE ACCOUNTING FOR THE VARIABILITY OF THE PHYSICAL PROPERTIES

3.1 *Calculation method of fragility curve*

Random numbers from a normal distribution were used to simulate the variability of the physical properties in the estimated amount of settlements. Then reliability analysis (Monte Carlo Simulation: MCS) was performed and evaluated as the fragility curve. The calculation method for the fragility curve related to the ground settlements during an earthquake was as follows:

1) Generate random numbers from a normal distribution (Figure 3). We generated 100 numbers and constructed a dataset with 100 cases of ground physical properties by referencing the actual survey and measurements of the dry density and moisture content as well as their means and standard deviations at the target location. For the dry density, the mean value was 1.60 g/cm^3 and the standard deviation was 0.068 g/cm^3. For the natural moisture content, the mean value was 20.0 % and the standard deviation was 2.90 %.

2) In the previous chapter 2(2), correlation equation α_1 was derived from the relationship between the initial dry density and volumetric strain, and α_2 from the relationship between the

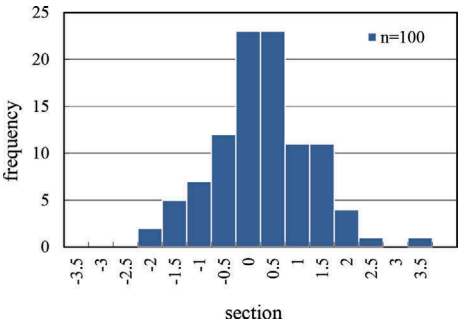

Figure 3. Normal distribution (100 numbers)

initial moisture content and volumetric strain. To calculate the amount of settlements accounting for the variability of physical properties, it is necessary to multiply these relationship formula by the equivalent volumetric strain curves (4), which were defined using the average physical properties (Kitazume et al.2015). This formula is shown in (3).

$$\varepsilon_v{}' = (\alpha_1 \cdot \alpha_2) \cdot \varepsilon_v \tag{3}$$

$$\varepsilon_v = \left[\frac{\tau_d}{(0.464\sigma_m{}' + 9.81)N^{-0.207}}\right]^{\frac{1}{0.355N^{0.0199}}} \tag{4}$$

Where $\varepsilon_v{}'$ (%) is the calculated volumetric strain accounting for the variability of characteristics, ε_v (%) is the volumetric strain calculated from the average physical properties obtained from formula (4), τ_d (kPa) is shear stress, σ'_m (kPa) is average confining stress, N is number of cycles and α_1 and α_2 are the relationship formula (1) and (2) from chapter 2.

3) Arbitrarily change the peak ground acceleration (PGA) of the seismic motion as an input for seismic response analysis and cumulative damage analysis. Then run 100 cases for each analysis. In this study, 100 cases of MCS were performed with the input seismic motion of PGA 680 Gal, whose amount of settlements was approximately 50 cm for the average physical properties (Kitazume et al. 2015). The same number of MCS was also performed with the input seismic motion just below and above this PGA (450 and 900 Gal).

4) Set arbitrary limit states (amount of settlements). For the 100 cases that estimated amount of settlements calculated from each PGA of seismic motion, find the probability of exceeding the limit states. In this study, we set 25, 50, and 100 cm as limit states.

5) For each limit state, assume a log-normal distribution for the probability data of exceeding the limit for three values of PGA seismic motion. Then derive cumulative distribution function (5), i.e., the fragility curve.

$$P_f(A) = \varphi\left(-\frac{\ln(A) - \ln(A_m)}{\zeta}\right) \tag{5}$$

Where $P_f(A)$ is the probability of damage related to amount of settlements, φ is the standard normal probability distribution function, A is PGA, A_m is the median of PGA, and ζ is the log standard deviation.

3.2 *Evaluation of the fragility curve*

Figure 4 shows the histogram of the estimated amount of settlements calculated for 100 cases using three types of PGA. The median, mean, and standard deviation assuming a log-normal distribution are shown. By applying the equivalent volumetric strain curves (4) with the average physical properties, the calculated amount of ground settlements during earthquakes was 50.6 cm. The median for the estimated values of PGA 680-Gal seismic motion of 100 cases was 59.8

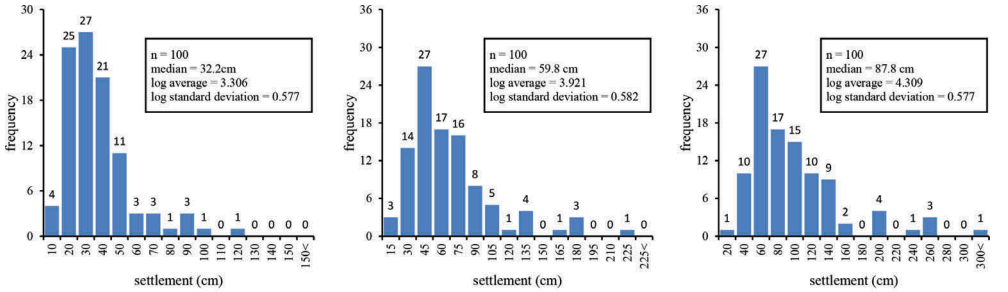

(a) PGA = 450 Gal (b) PGA = 680 Gal (c) PGA = 900 Gal

Figure 4. Histogram of the estimated amount of settlements for 100 cases using three types of PGA.

Table 2. Probability of exceeding for each limit state

Limit state [settlement (cm)]	PGA (Gal)	Probability of exceeding
25	450	0.54
	680	0.90
	900	0.97
50	450	0.12
	680	0.51
	900	0.77
100	450	0.01
	680	0.10
	900	0.30

Table 3. Statistical values for each fragility curve (log normal distribution assumed)

Limit state [settlement] (cm)	Median (Gal)	Log standard deviation	Average (Gal)	Coefficient of variation
25	433.8	0.357	462.4	0.369
50	680.4	0.364	727.2	0.377
100	1093.9	0.372	1172.2	0.385

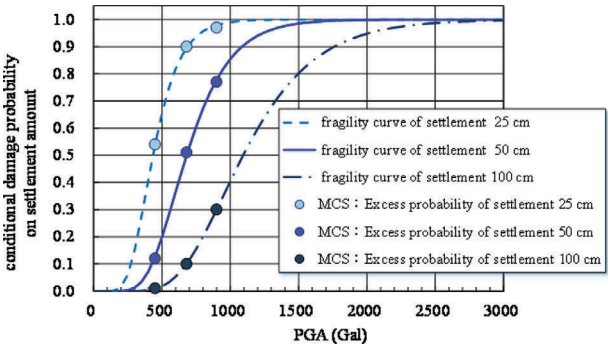

Figure 5. Fragility curves for each limit state (settlement)

cm. The PGA 450-Gal seismic motion showed a median of 32.2 cm for the 100 estimated cases, and the PGA 900-Gal seismic motion showed a median of 87.8 cm for the 100 estimated cases.

Table 2 shows the probability of exceeding the limit states calculated from the MCS results with three types of PGA seismic motions. Figure 5 shows the fragility curves by limit states calculated from a regression calculation assuming a log-normal distribution. Table 3 shows the statistical values. By focusing on the difference in the limit states, the fragility curves are located from the left in an increasing order of the settlements amount, as expected. Therefore, the conditional probability exceeding the limit becomes higher. When the limit state is set higher, the curvature of the fragility curve becomes more gradual, indicating a larger variation in the estimated amount of settlements.

4 FRAGILLITY CURVE ACCOUNTING FOR MODELING ERRORS

4.1 *Seismic response analysis methods used to estimate amount of settlements*

The amount of settlements was estimated using four types of seismic response analysis methods (Table 4). They are a) the equivalent linear analysis based on multiple reflection theory, b)

Table 4. Four types of seismic response analysis methods

Seismic response analysis method		
a)	Equivalent linear analysis	(multiple reflection theory)
b)	Nonlinear FEM analysis	(R-O stress-strain model)
c)	Nonlinear FEM analysis	(H-D stress-strain model)
d)	Nonlinear FEM analysis	(multispring model)

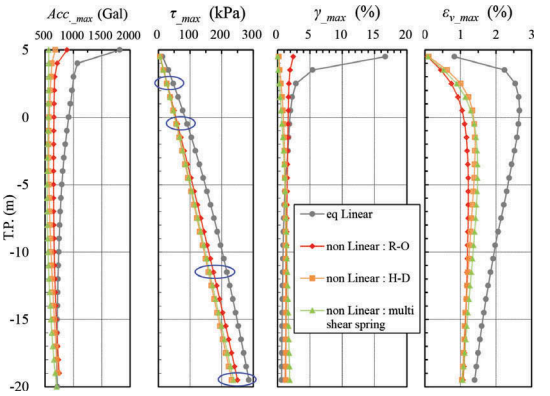

Figure 6. Depth distribution of the maximum response value

nonlinear FEM analysis (Ramberg-Osgood (1964) stress-strain model), c) nonlinear FEM analysis (Hardin-Drnevich (1972) stress-strain model), and d) nonlinear FEM analysis (multispring model (Towhata and Ishihara. 1985)). The same analysis code was used for b) and c).

Figure 6 shows the acceleration, the depth distribution of the maximum response value of shear stress and strain, and the depth distribution of the volumetric strain calculated by the cumulative damage analysis using the four types of earthquake response analyses. The total of the maximum (remaining) volumetric strain is the amount of ground surface settlements.

The circles in Figure 6 show the time series of shear stress calculated from these four seismic response analyses using four depth values (elm03, elm06, elm17 and elm25), and Figure 7 shows the section between 5 to 25 seconds. All four shear stress graphs have similar shapes and the numbers of cycles are about the same. However, for the amplitude of the shear stress corresponds to so-called a "killer pulse" section, the equivalent linear analysis shows a greater depth compared to other nonlinear FEM analyses regardless of the depth. This is especially pronounced at a shallower depth. This result shows that the equivalent linear analysis calculates a greater volumetric strain.

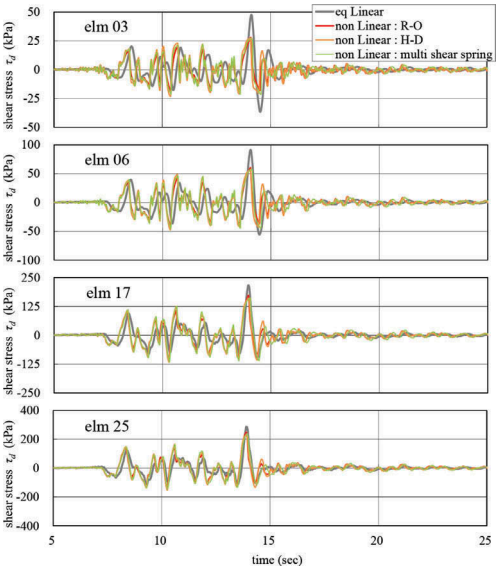

Figure 7. Shear stress (τ_d) time history

4.2 *Modeling errors*

The modeling error characteristics are shown below by replicating the expression method of Otake and Honjo (2014) using *bias* and *COV* as indices. The mean of the measurement value A divided by the calculated value B (A/B) is called the *bias*. The *bias* shows the calculated value against the measurement value. *COV*, which is a variable coefficient that is defined as the standard deviation of A/B divided by the *bias*, is an index to express the size of error by normalizing the *bias*.

In this study, the measurement value A was the actual measured amount of settlements of backfilled unsaturated sandy soil inside the nuclear power plant after the 2007 Niigata-ken Chuetsu-oki Earthquake. We used a median value of 35 cm from the actual measured settlements between 30 to 40 cm (Kitazume et al. 2015). The calculated value B was the estimated settlements obtained from the cumulative damage analysis using the time history of shear stress derived from each method of seismic response analysis.

Table 5 shows the estimated settlements and the characteristics of modeling errors. The equivalent linear analysis estimated settlements as 50.6 cm, which is a slight overestimate of the actual measurement value. The nonlinear FEM analysis methods estimated settlements as 26.7 to 30.3 cm, which are slight underestimates of the actual measurement value. The indices describing the characteristics of the modeling error in estimating settlements during earthquakes for unsaturated sandy soil using these four analyses yield *bias* = 1.09 and *COV* = 0.25.

The results above show the modeling errors from this study. The results reflect difference among these four types of seismic response analysis methods. These numerical values cannot be generalized. However, the resulting variation can be considered small (*COV* = 0.25), although it is an estimation of the displacement reflecting the effects of the nonlinear characteristics and seismic motion characteristics (duration and existence of killer pulse) of the ground.

Let the calculated coefficient of variation *COV* = 0.25 be approximated by the value of log standard deviation β_u (*COV* 0.25 ≒ β_u). Figure 8 shows the composite log standard deviation at each limit state, where β_r is the randomness of the ground physical properties values, β_u is the modeling error, and β_c is composite log standard deviation, i.e. $(\beta_r^2+\beta_u^2)\text{^}0.5$. Figure 8 shows the composite fragility curve for each limit state. Comparing the fragility curve that

Table 5. Estimated settlements and modeling errors

Analysis method	Measured settlements A (cm)	Estimated settlements B (cm)	A/B	*bias*	*COV*
a)	35	50.6	0.69	1.09	0.25
b)		26.7	1.31		
c)		29.3	1.19		
d)		30.3	1.16		

Limit state [settlement] (cm)	Median (Gal)	β_r	β_c
25	433.8	0.357	0.369
50	680.4	0.364	0.377
100	1093.9	0.372	0.385

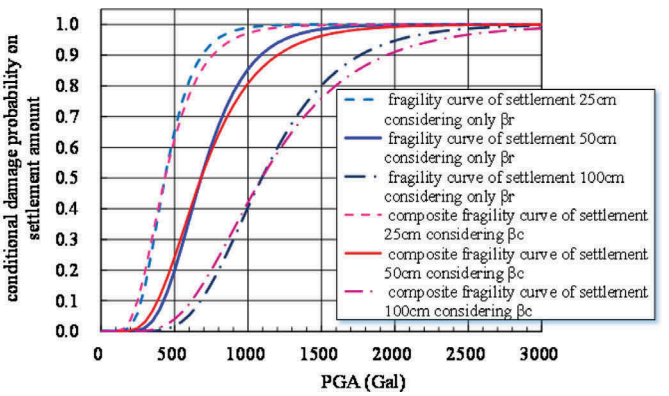

Figure 8. Composite fragility curves for each limit state (settlement)

only accounts for the variability of ground physical properties (random variability: β_r) to the composite fragility curve, the composite curve has a more gradual slope.

5 CONCLUSION

This study led to the following conclusions:

1. Smaller is the initial dry density of unsaturated sandy soil, higher is the volumetric strain arising from cyclic shear. Besides, higher is the initial moisture content, higher is the volumetric strain.
2. When shear stress ratio differs, percentage change in volumetric strain due to difference in initial dry density and initial moisture content also differs.
3. We calculated the fragility curve using MCS to estimated settlements during an earthquake by accounting for the variability of dry density and moisture content. The larger the limit state, the more gradual the slope of the fragility curve becomes and the higher the variability of the estimated settlements.
4. On the modeling errors related to the estimated settlements during an earthquake for unsaturated sandy soil, we considered analysis methods and model fits in relation to the settings for the Rayleigh damping for nonlinear analyses and parameters for ground shear stress model. Nevertheless, as the model parameters are set by the discretion of the organization or analyst, the estimated values are expected to fluctuate more than the results in this study.

REFERENCES

Sakai, T., Suehiro, T., Tani, T. & Sato, H. 2009. Geotechnical performance of the Kashiwazaki-Kariwa Nuclear Power Station caused by the 2007 Niigataken Chuetsu-oki earthquake, *Case History Volume for Performance-Based Design in Earthquake Geotechnical Engineering*, Technical Committee No.4, ISSMGE, pp.1–29.

Kitazume, T., Goto, S., Araki, K., Sato, H. & Sato, M. 2015. Volumetric compression characteristics of unsaturated sandy soils under cyclic shear for estimation of settlement, *6th International Conference on Earthquake Geotechnical Engineering*.

Jennings, P. C. 1964. Periodic response of a general yielding structure, *Proc. ASCE*, EM2, pp.131–163.

Hardin, B. O. and Drnevich, V. P. 1972. Shear modulus and damping in soils: Design equations and curves, *J. SMFD, Proc. ASCE*, Vol.98, No.SM7, pp.667–692.

Towhata, I., and Ishihara, K. 1985. Modeling soil behavior under principal stress axes rotation, *Proc. 5th International conference of numerical method in geotechnical*, Nagoya, Vol.1, pp.523–530.

Otake, Y., and Honjo, Y. 2014, Characterization of model error in geotechnical structural design, *Journal of JSCE(C)*, Vol.70, No.2, pp.170–185. (in Japanese)